



# Effects of varying local temperature on the optical properties of cells in-vitro



Iftikhar Ahmad<sup>a,b,\*</sup>, Abdul Rehman<sup>a</sup>, Junaid A. Khan<sup>a</sup>,  
Muhammad Rafi<sup>a</sup>, Ahmat Khurshid<sup>a</sup>, Hasan Nisar<sup>a</sup>, S.S.Z. Zaidi<sup>c</sup>,  
Masroor Ikram<sup>a</sup>

<sup>a</sup> Pakistan Institute of Engineering and Applied Sciences (PIEAS), Nilore, 45650, Islamabad, Pakistan

<sup>b</sup> Center for Nuclear Medicine and Radiotherapy (CENAR), Brewery Road, P.O. Box 17, Quetta, Pakistan

<sup>c</sup> National Institute of Health, Park Road, Islamabad, Pakistan

Available online 11 June 2015

## KEYWORDS

Biomedical;  
Optical properties;  
Absorption  
coefficient;  
Scattering  
coefficient;  
Anisotropy factor

**Summary** Summary Increase in local temperature during light exposure of biological tissues plays an important role in determining the fate of most therapeutic modalities. Variations in the optical properties (absorption coefficient, scattering coefficient, anisotropy factor, optical depth etc.) of two cancer cell lines “Rhodomyosarcoma and Cervical carcinoma” due to gradual increase in temperature were determined quantitatively with a double integrating sphere system. It was observed that all three coefficients showed decreasing tendency as the temperature increases for both the cell lines except for scattering coefficient of HeLa which remain constant within error limit. Anisotropy factor for both cell lines increased indicating temperature dependent subcellular density variations. Temperature dependent optical properties information may lead to precise dosimetry and could help clinicians for predicting the therapeutic modality outcome.

© 2015 Elsevier B.V. All rights reserved.

## Introduction

Optical properties of biological tissues are essential for understanding light absorption and distribution. Biochemical composition of investigated tissue can be probed from

light absorption while light scattering provides information about its micro-architecture. Fairly prominent contrast in the optical properties of pathological and normal tissues has potentially opened new optical diagnostic techniques [1–8]. Likewise intensive analysis of the efficacy of many optical therapeutic modalities reveal the particular importance of optical properties [4,9,10]. Consequently, there is growing interest in the measurement of optical properties for light dosimetry in the biomedical research and applications.

Tissue optical properties may change during the course of optical therapeutic procedure due to thermally induced changes at elevated temperatures as indicated by many studies [11–13]. For instance, the absorption coefficient and anisotropy factor were observed to decrease while

\* Corresponding author at: Pakistan Institute of Engineering and Applied Sciences (PIEAS), Islamabad, Pakistan.  
Tel.: +92 3339234347; fax: +92 512208070.

E-mail addresses: [iahmadmp@gmail.com](mailto:iahmadmp@gmail.com) (I. Ahmad), [abdulrehmanphy01@gmail.com](mailto:abdulrehmanphy01@gmail.com) (A. Rehman), [fac268@pieas.edu.pk](mailto:fac268@pieas.edu.pk) (J.A. Khan), [ahmat82@gmail.com](mailto:ahmat82@gmail.com) (A. Khurshid), [hasanisar@gmail.com](mailto:hasanisar@gmail.com) (H. Nisar), [masroor@pieas.edu.pk](mailto:masroor@pieas.edu.pk) (M. Ikram).

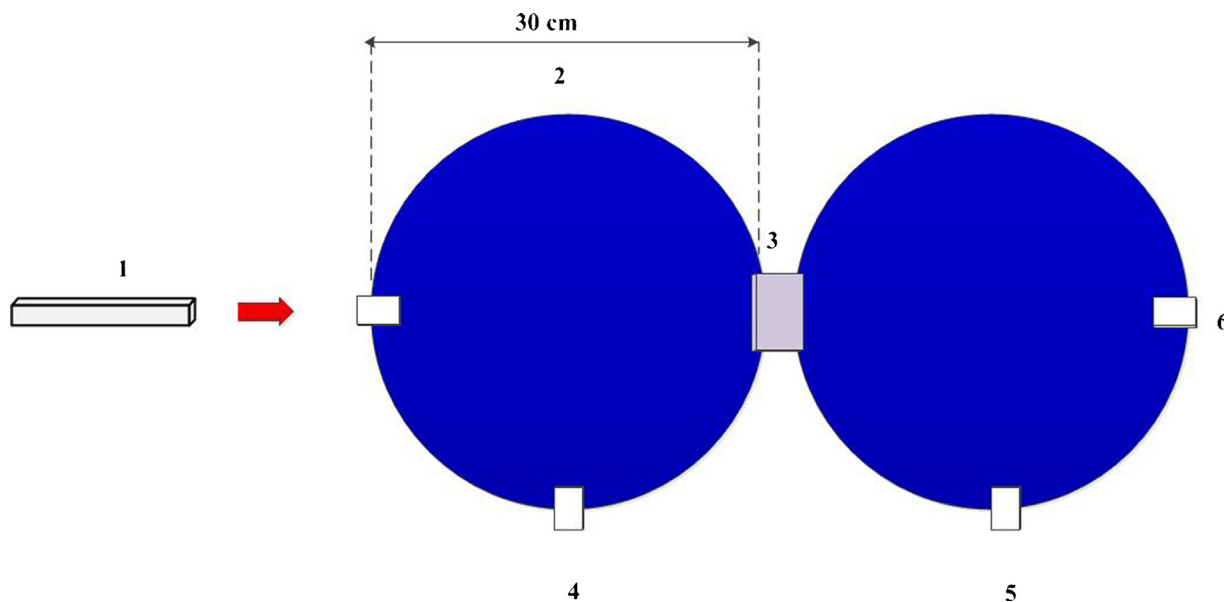


**Figure 1** Experimental setup for optical properties determination of RD and HeLa cells. 1 = HeNe Laser; 2 = Integrating Sphere; 3 = Sample; 4 = Detector port for  $R_d$ ; 5 = Detector port for  $T_d$ ; 6 = Detector port for  $T_c$ .

scattering coefficient increased with increasing temperatures for *ex vivo* measurements of rat prostate [11]. Variations in parameters like tissue hydration, pH and photochemical changes like denaturation and coagulation are also influenced by an elevation in temperature [14,15].

Optical properties (absorption coefficient ( $\mu_a$ ), scattering coefficient ( $\mu_s$ ) and anisotropy parameter ( $g$ )) have been determined with different techniques like diffuse reflectance, single and double integrating spheres method, elastic scattering, sized fiber reflectometry, oblique incidence optical fiber reflectometry etc., for various biological samples like human blood, liver, colon, prostate, small intestine, nasal cartilage, brain, skin muscle and fat has been studied for their optical properties [16–25]. All these studies investigated the optical properties of biological tissue *in vivo* or *ex vivo*. However, no report is available for *in vitro* measurements that quantify the changes in optical properties with temperature to the best of our knowledge. *In vitro* studies are of particular interest in biomedical research as these investigations provide fascinating grounds for more realistic models, preliminary analysis and provoke the opportunity for optimizing various parameters. For instance, light dosimetry and optimization in photodynamic therapy (PDT) fit in the framework of *in vitro* studies. Therefore, *in vitro* measurement of optical properties and its temperature dependence would find many applications in optical theranostic modalities [26].

The goal of this study is to investigate the effect of temperature on optical properties of Rhabdomyosarcoma (RD) and cervix adenocarcinoma (HeLa) cells. The widely used double integrating sphere technique was utilized for measurement of optical properties at various temperatures. This technique offers many advantages such as simultaneous light collection at both reflected and transmitted arms and spatial integration. Detector saturation problems are avoided when dealing with highly collimated sources such as lasers. Further, cell suspension samples were measured in a quartz

cuvette (1 cm path length) so that thickness of each sample was uniform in all cases.

## Material and method

### Experimental setup

The well-established and widely used integrating-sphere technique was employed for the measurement of optical properties of HeLa and RD cells. The experimental setup is schematically shown in Figure 1. The samples were placed sequentially in the holder between the double integrating spheres of 30 mm diameter and 3 mm detector port (Optoprism, Germany). The samples were illuminated with a HeNe laser of 2 mm beam diameter, 0.84 mrad divergence and 0.95 mW power (Spindler & Hoyer, Germany). The light after interacting with sample was collected by integrating spheres. The diffuse reflected and total transmitted light fluence was measured by spectrometer coupled with integrating spheres (Avantes, Avaspec-2048, The Netherlands). Collimated transmission was measured at 3 m away from the sample to exclude the scatter fraction from the primary beam [27]. Optical properties were computed by using inverse adding doubling (IAD) algorithm.

### Sample preparation

Human cervix adenocarcinoma (HeLa) and Rhabdomyosarcoma (RD) cell lines were cultured and maintained in modified Eagle's medium (MEM) containing 10% FBS, 200 mM L-glutamine, 100 U/ml penicillin and 100 mg/ml streptomycin (Sigma-Aldrich). The cells were cultured at 37 °C in a humidified atmosphere with 5% CO<sub>2</sub>. Cells were resuspended in MEM upon achieving 80% confluency in cell culture flasks. Cell density was determined with Hemocytometer. HeLa cells density of  $1.69 \times 10^5$  /ml and RD cells  $6.49 \times 10^5$  /ml was

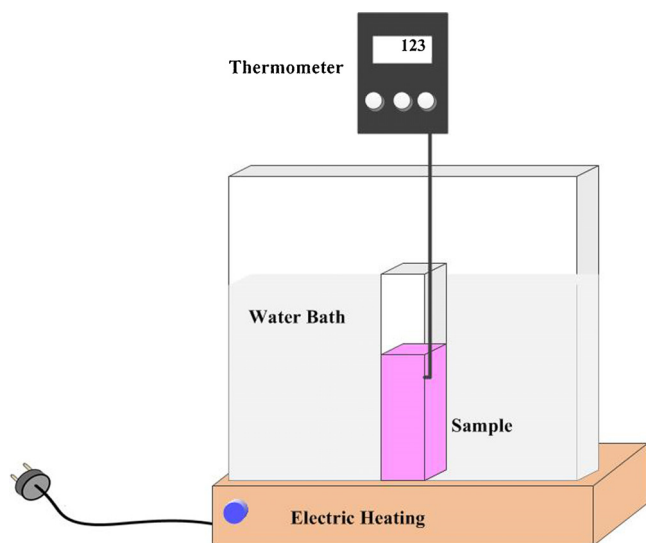


**Figure 2** Schematic of electric heating used for temperature elevation of the samples.

carried for further experiments. Temperature of the sample was increased (from 20 to 60°C with 5 degree step) with electrically heated water bath coupled with thermometer as shown in Figure 2.

## Measurements

Diffuse reflectance and total transmittance values for the two cell culture suspension were measured with double integrating sphere. Freshly coated barium sulfate ( $\text{BaSO}_4$ ) plate served as reference for calibration of integrating spheres. Diffuse reflectance ( $R_d$ ) of the sample can be estimated in terms of sample, standard and background reflectance as follows:

$$R_d = \frac{R_{(s)} - R_{(0)}}{R_{(std)} - R_{(0)}}$$

where,  $R_{(s)}$  and  $R_{(std)}$  are the light intensities measured by reflectance sphere with sample and standard barium sulphate plate respectively.  $R_{(0)}$  is the background light intensity detected without any sample. Transmittance of the sample can be determined by,

$$T_d = \frac{T_{(s)} - T_{(0)}}{T_{(0,1)} - T_{(0)}}$$

where,  $T_{(s)}$  and  $T_{(0,1)}$  are the light intensities measured by transmittance sphere with the sample and barium sulphate plate in sample holder respectively.  $T_{(0)}$  is the background light intensity detected without any sample.

Collimated transmittance  $T_c$  was measured at 3 m distance from the sample by

$$T_c = \frac{T_{(s)}}{T_{(0)}}$$

where,  $T_{(s)}$  and  $T_0$  are measured intensities with sample and without sample respectively.

The widely used computational model (inverse adding doubling, IAD algorithm) was employed to calculate all three optical properties (scattering coefficient, absorption coefficient and anisotropy factor) of the investigated samples. These calculations are essentially based on the experimentally measured quantities of diffuse reflectance, total transmittance, collimated transmittance [28]. This technique also accounts for the optical beam parameters such as size of the incident beam, refractive index of sample and geometrical configurations of the experiment like integrating sphere and its ports dimensions. The refractive index for the samples was measured experimentally using the diffraction method and employed in the IAD algorithm. Refractive index for HeLa cells was 1.345 while 1.341 for RD cells. Then the temperature dependence of total attenuation coefficient ( $\mu_t$ ), optical depth ( $\tau$ ) and albedo ( $\alpha$ ) from the measured optical properties were calculated using the following relations:

$$\mu_t = \mu_a + \mu_s$$

$$\tau = d\mu_t$$

$$\alpha = \mu_s/\mu_t$$

where,  $d$  is the physical thickness (1 cm) of the sample.

## Results

Temperature dependence of diffuse reflectance, total transmittance and collimated transmittance for HeLa and RD cells is shown in Figure 3a and b, respectively. Each numerical value depicted in Figure 3 corresponds to the mean value over three readings of all samples. The mean values were employed in IAD for computing optical properties. Closer examination of both graphs indicates that increase in total transmittance is more prominent than diffuse reflectance for both types of cells. Unlike HeLa cells, the collimated transmittance decreased as a function of temperature for RD cells.

Figure 4a and b shows the variations in absorption coefficient ( $\mu_a$ ), scattering coefficient ( $\mu_s$ ) and total attenuation coefficient ( $\mu_t$ ) as a function of temperature for HeLa and RD cells respectively. Analysis and comparison of Figure 4a and 4b) reveals many interesting features: Obviously, all three coefficients decrease with increasing temperature.  $\mu_s$  falls more rapidly as compared to ( $\mu_t$ ) for both types of cells. Abrupt decrease in both  $\mu_a$  and  $\mu_s$  is observed at initial rise of temperature. Decrease in all three attenuation coefficients of RD cells are fairly pronounced compared to HeLa cells. Almost no change in attenuation coefficients for HeLa cells at higher studied temperatures was observed.

To better illustrate the dependence of attenuation coefficients on temperature, we have shown the percentage change as a function of temperature in Figure 5a and b for HeLa and RD cells respectively. Attenuation coefficients at 20°C were supposed as reference for calculating percent change in all three coefficients. It can be observed that the behavior of change in the scattering and total attenuation

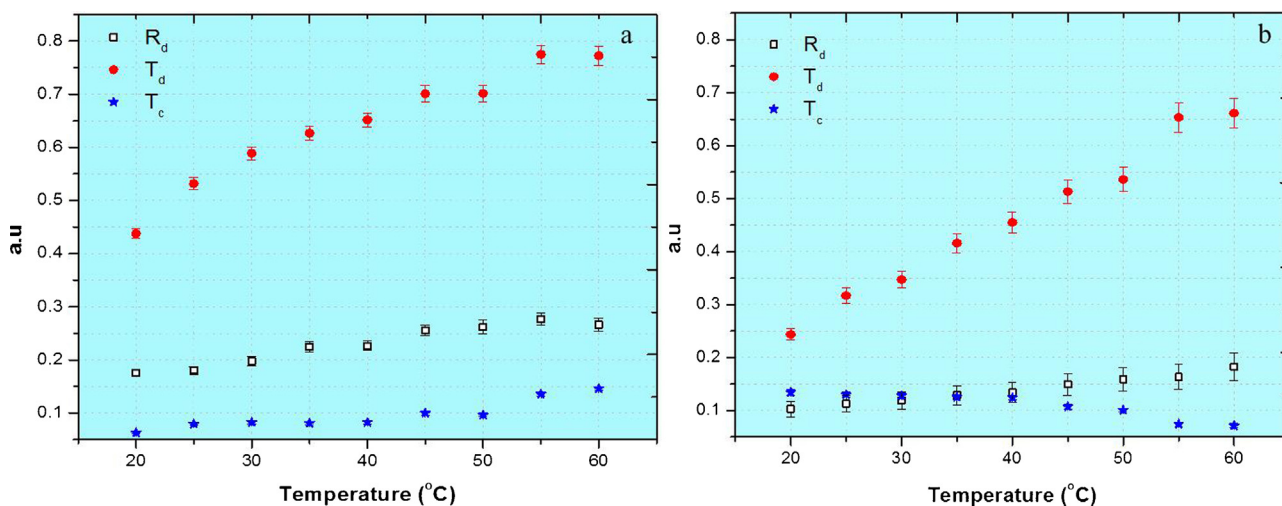


Figure 3 Variations of  $R_d$ ,  $T_T$  and  $T_c$  with temperature for (a) HeLa and (b) RD cells.

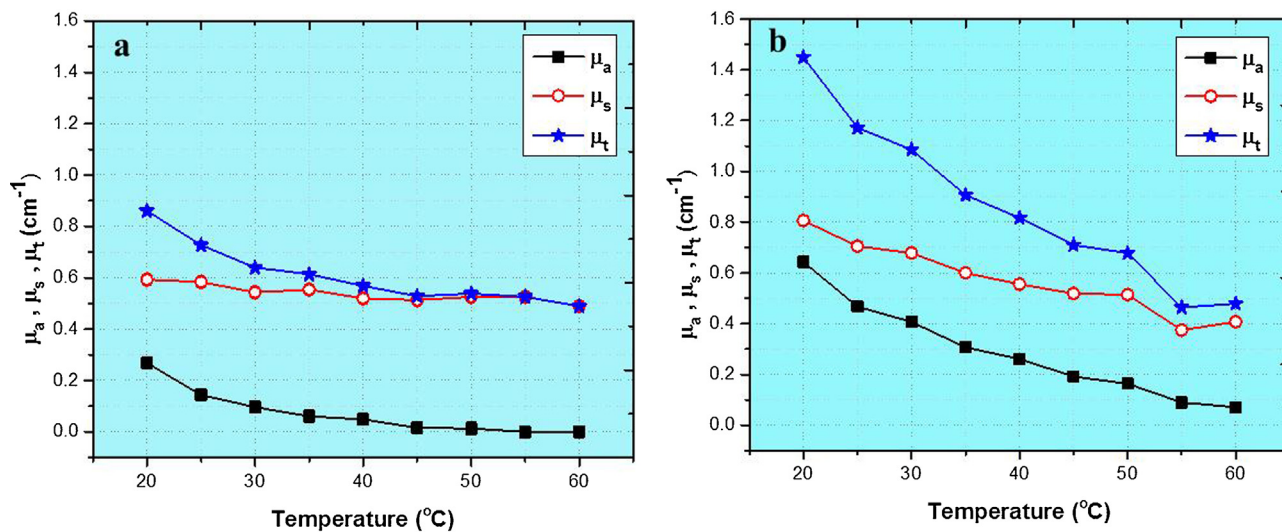


Figure 4 Variations of absorption, scattering, and total coefficients with temperature for (a) HeLa and (b) RD cells.

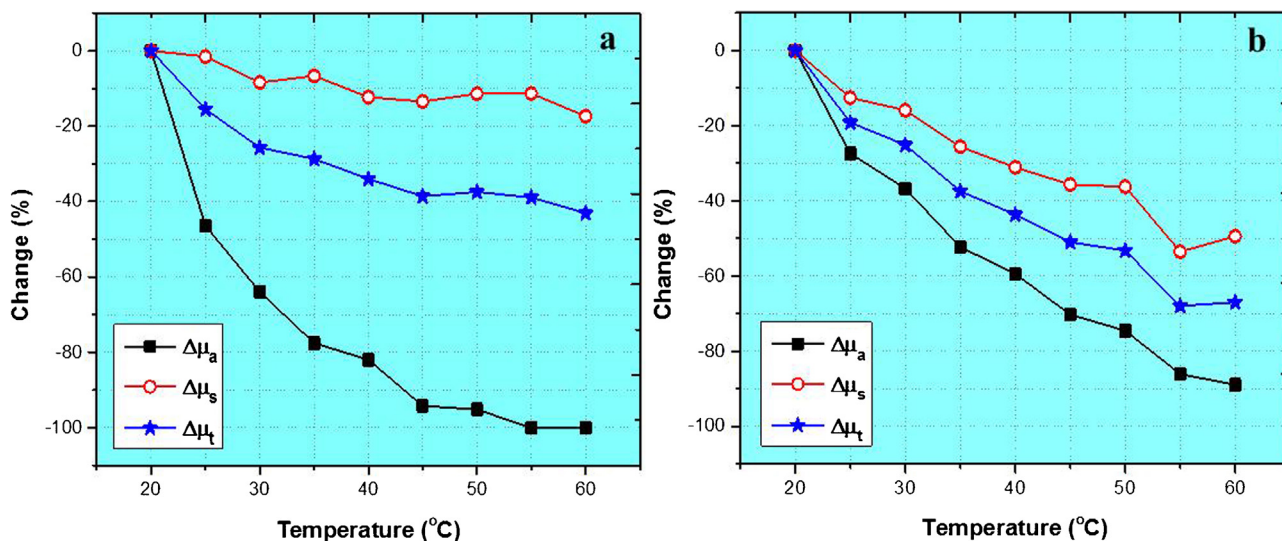


Figure 5 Percentage changes of absorption, scattering, and total coefficients with temperature for (a) HeLa and (b) RD Cells.

**Table 1** Variations of  $g$  with temperature for RD and HeLa Cells.

Temperature ( $^{\circ}\text{C}$ )	Estimated $g$ for HeLa Cells	Change (%)	Estimated $g$ for RD Cells	Change (%)
20	0.755	0	0.486	0
25	0.758	0.4	0.525	8.03
30	0.767	1.6	0.565	16.3
35	0.767	1.6	0.643	32.3
40	0.781	3.4	0.68	39.9
45	0.789	4.5	0.735	51.2
50	0.798	5.7	0.748	53.9
55	0.827	9.6	0.845	73.8
60	0.835	10.6	0.836	72.1

coefficients is very similar for both types of cells. However decrease in absorption coefficient for RD cells is hardly visible as compared to the pronounced decrease in HeLa cells. Unlike scattering coefficient, the anisotropy factor progressively increased from 0.486 to 0.836 over the complete temperature range for RD cells representing an increase of 72% as shown in Table 1. The corresponding increase for HeLa cells was less prominent ( $\sim 10\%$ ). Biological tissues are generally believed to be highly forward scattering ( $g > 0.8$ ). Results of the conducted experiment follow a similar trend. Further the increase in forward scattering with temperature can be attributed to the dynamics of protein denaturation and coagulation [14,29,30].

Two additional important parameters, optical depth  $\tau$  and albedo  $\alpha$  were computed from the experimentally determined attenuation and scattering coefficients and shown in Figure 6a and b. The relative contribution to attenuation from absorption or scattering is described by albedo  $\alpha$  while the optical depth  $\tau$  is a dimensionless parameter that scales the physical thickness of sample to "optical thickness" in terms of light interaction with sample. Optical depth essentially describes the limits on light penetration in tissue. The extreme case of  $\alpha = 1$  represent scattering only while for  $\alpha = 0$  attenuation is restricted to absorption only. There is no such constraint impose on the possible values of  $\tau$ . Starting values of  $\alpha > 0.5$  at  $20^{\circ}\text{C}$  for both cell types suggest that scattering is the dominant process of attenuation compared to absorption. The albedo increase by 45% and 53% for HeLa and RD cells respectively. Figure 6a and b illustrates a similar decreasing trend for optical depth as a function of temperature for both samples. However, an interesting observation from closer inspection is the almost two fold decrease in optical depth for RD cells compared to HeLa cells.

## Discussion

The attenuation of the incident laser light in turbid media like biological cells and tissues primarily depend on wavelength of the incident light and characteristics of scattering particles like its size, shape, density, and packing etc., in the sample [4,31]. In this study, temperature of the sample (cell suspension) was raised keeping the light source constant. Therefore effect of temperature elevation in terms of changes in optical properties can be investigated. Such changes in optical properties are important in many areas of

biomedical research especially in laser therapies where laser beam intensity, treatment duration, and number of treatment fraction may be determined by the rate of change of the scattering and absorption coefficients [9,32,33].

Temperature dependent changes in the optical properties of HeLa and RD cells can be correlated to the changes in microarchitecture and morphology of cells. We assume that the denaturation and coagulation of various cellular structural proteins may be responsible for the alteration in optical properties. The imparted thermal energy is employed to disrupt and break the weak bonds that are responsible for the tertiary and quaternary integrity in proteins [9,30,34]. Another line of argument in favor of decreasing coefficients may come from the chromophore denaturation that occurs at elevated temperatures [29,35]. Some studies offered an alternative explanation attributing these changes in optical properties to tissue shrinkage caused by a loss of water during heating [9,34]. Lastly, presence of glycol-lipids in cell membranes may also contribute to the observed negative temperature coefficient of scattering of both cells. The gel phase of membrane glycol-lipids is converted to crystalline phase and then liquid crystalline phase with increasing temperature. This increase in fluidity indicates the disordered phase of glycol-lipids [36,37]. Thus, we may conclude that perhaps the phase transition of glycol-lipids also contributes to the decrease in scattering.

It is also important to note that the energy imparted to the sample from heating possess a temperature and time dependence. Agah et al. suggested that changes in optical properties occur in two phases; a fast temperature-dependent process up to  $70^{\circ}\text{C}$  and a slow temperature-independent process above  $70^{\circ}\text{C}$  [35]. However, attesting the essential interpretation for the dominant features of in vitro experimental data is seemingly missing. Nevertheless, elucidation of the temperature dependent dynamics of optical properties should be a priority due its importance in biomedical research.

The interesting observation evolved from inspection of Figure 5a and b is that the starting values and the decrease in all three coefficients with temperature were higher for RD cells compared to HeLa cells. These observations probably indicate the distinguishing features of both cells in terms of different origins. RD cells are derived from pelvic rhabdomyosarcoma biopsy specimens with embryonal histology while HeLa cells are derived from human cervical

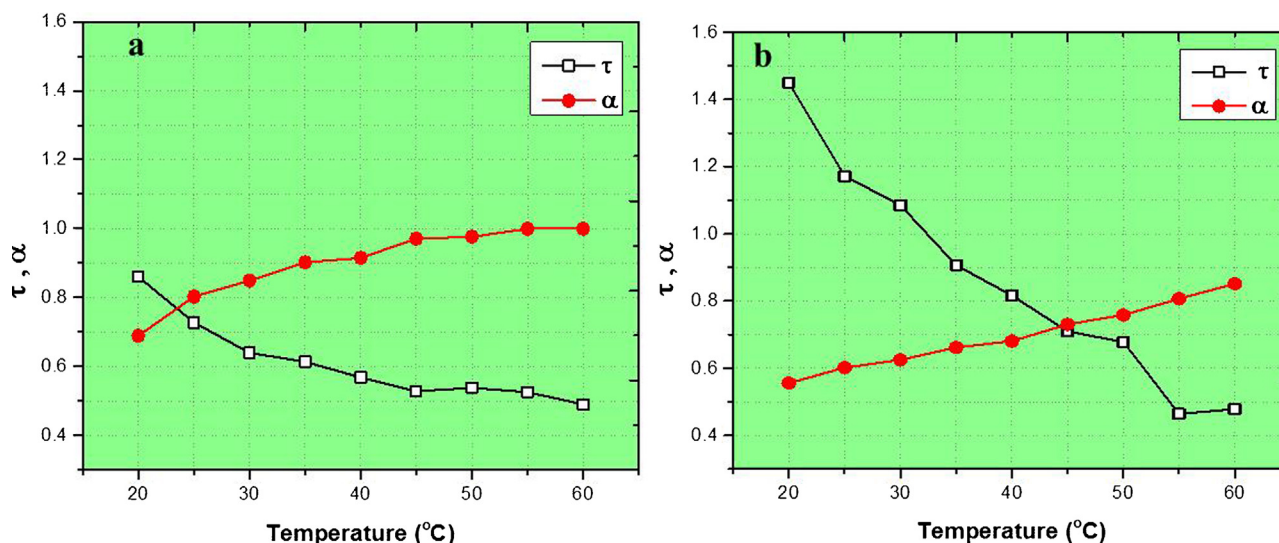


Figure 6 Variations of optical depth and albedo with temperature for (a) HeLa and (b) RD cells.

adenocarcinoma. In contrast to HeLa cells, RD cells display protein abundance primarily arising from their muscular nature. Distinct manifold expression of proteins like actin, myosin, tropomyosin, troponin, and myomesin etc., by muscle (RD) cells essentially provide muscle contraction, cytoskeleton, and cells migration etc., [38–40]. Protein abundance triggers multiple denaturation and coagulation cascades that significantly affect optical properties including absorption and scattering. Another line of argument in convincing the relatively higher scattering of RD cells can probably be assign to the scattering properties of the most dominant micron sized structure of RD cells; the mitochondria. RD cells seem to have much higher density of mitochondria that will present intense Rayleigh scattering [41]. Furthermore, Rd cells express elevated levels of chromophores such as myoglobin compared to HeLa cells.

The albedo increase and decrease in optical depth with temperature permits its description in terms of dominant scattering relative to absorption. Both scattering and absorption contribute towards albedo and optical depth of the medium. However, the gradual increase in albedo can be associated with the prominent decrease in absorption compared to scattering. On the other hand, decreasing scattering and absorption attests the subsequent decrease in optical depth.

## Conclusion

Temperature elevation led to significant changes in the optical properties of HeLa and RD cells. Absorption and scattering coefficients and optical depth decreased while anisotropy factor and albedo increased as a function of temperature. Dynamics of protein denaturation may have provoked these changes. Despite the abundant accumulated experimental work available on individual tissue samples, light dosimetry for the safe and effective biomedical procedures remains a challenge. Further, our results demonstrate the need to exercise caution in attempting extrapolating data obtained from *in vitro* to *in vivo* experiments.

## Acknowledgments

The authors thank Mr. Aziz ul Reham of National Institute of Laser and Optonics, Pakistan for his kind help and suggestions during the experiment. Support of Institute of Biomedical and Genetic Engineering, Pakistan is highly appreciated. The research was funded by IT and Telecom Endowment Fund, PIEAS, Pakistan.

## References

- [1] Svensson T, Andersson-Engels S, Einarsdóttir M, Svanberg K. In vivo optical characterization of human prostate tissue using near-infrared time-resolved spectroscopy. *J Biomed Opt* 2007;12(1):014022.
- [2] Salomatina E, Jiang B, Novak J, Yaroslavsky AN. Optical properties of normal and cancerous human skin in the visible and near-infrared spectral range. *J Biomed Opt* 2006;11(December):1–9.
- [3] Abookasis D, Lay CC, Mathews MS, Linskey ME, Frostig RD, Tromberg BJ. Imaging cortical absorption, scattering, and hemodynamic response during ischemic stroke using spatially modulated near-infrared illumination. *J Biomed Opt* 2009;14(2):024033.
- [4] Jacques SL. Optical properties of biological tissues: a review. *Phys Med Biol* 2013;58(11):R37–61.
- [5] Gebhart SC, Lin WC, Mahadevan-Jansen A. In vitro determination of normal and neoplastic human brain tissue optical properties using inverse adding-doubling. *Phys Med Biol* 2006;51(8):2011–27.
- [6] Hohmann A, Voit F, Schäfer J, Kienle A. Multiple scattering of polarized light: influence of absorption. *Phys Med Biol* 2014;59(11):2583–97.
- [7] Bashkatov AN, Genina EA, Kochubey VI, Rubtsov VS, Kolesnikova EA, Tuchin VV. Optical properties of human colon tissues in the 350–2500 nm spectral range. *Quantum Electron* 2014;44(8):779–84.
- [8] Rehman A, Ahmad I, Rehman K, Anwar S, Firdous S, Nawaz M. Optical properties measurement of highly diffusive tissue phantoms for biomedical applications. *Laser Phys* 2015;25(2):025605.

- [9] Ritz JP, Roggan A, Germer CT, Isbert C, Mu G, Buhr HJ. Continuous changes in the optical properties of liver tissue during laser-induced interstitial thermotherapy. *Lasers Surg Med* 2001;312:307–12.
- [10] Sandell JL, Zhu TC. A review of in-vivo optical properties of human tissues and its impact on PDT. *J Biophotonics* 2011;4(11–12):773–87.
- [11] Skinner MG, Everts S, Reid AD, Vitkin IA, Lilge L, Sherar MD. Changes in optical properties of ex vivo rat prostate due to heating. *Phys Med Biol* 2000;45(5):1375–86.
- [12] Laufer J, Simpson R, Kohl M, Essenpreis M, Cope M. Effect of temperature on the optical properties of ex vivo human dermis and subdermis. *Phys Med Biol* 1998;43(9):2479–89.
- [13] Hayward JE, Bruulsema JT, Patterson MS, Essenpreis M. In vivo temperature dependence of human skin optical properties in the NIR—Osa Technical Digest. *Biomed Optics* 1999:ATuA3.
- [14] Pearce J, Thomsen S. Optical-thermal response of laser-irradiated tissue. Boston, MA: Springer US; 1995. p. 561–606.
- [15] Cletus B, Künemeyer R, Martinsen P, McGlone VA. Temperature-dependent optical properties of Intralipid measured with frequency-domain photon-migration spectroscopy. *J Biomed Opt* 2010;15(5):017003.
- [16] Cappon DJ, Farrell TJ, Fang Q, Hayward JE. Fiber-optic probe design and optical property recovery algorithm for optical biopsy of brain tissue. *J Biomed Opt* 2013;18(10):107004.
- [17] Yuzhakov AV, Sviridov AP, Baum OI, Shcherbakov EM, Sobol EN. Optical characteristics of the cornea and sclera and their alterations under the effect of nondestructive 1.56-m laser radiation. *J Biomed Opt* 2013;18(5):58003.
- [18] Rosen J, Suh H, Giordano N, A'amar O, Rodriguez-Diaz E, Bigio I, Lee S. Preoperative discrimination of benign from malignant disease in thyroid nodules with indeterminate cytology using elastic light-scattering spectroscopy. *IEEE Trans Biomed Eng* 2013;61(8):2336–40.
- [19] Friebe M, Helfmann J, Netz U, Meinke M. Influence of oxygen saturation on the optical scattering properties of human red blood cells in the spectral range 250 to 2000 nm. *J Biomed Opt* 2009;14(3):034001.
- [20] Yu Y, Xiao C, Chen K, Zheng J, Zhang J, Zhao X, et al. Different optical properties between human hepatocellular carcinoma tissues and non-tumorous hepatic tissues in vitro. *J Huazhong Univ Sci Technol Med Sci* 2011;31(4):515–9.
- [21] Ao H, Xing D, Wei H, Gu H, Wu G, Lu J. Thermal coagulation-induced changes of the optical properties of normal and adenomatous human colon tissues in vitro in the spectral range 400–1100 nm. *Phys Med Biol* 2008;53(8):2197–206.
- [22] Wei H-J, Xing D, He B-H, Wu R-H, Gu H-M, Wu G-Y, et al. Absorption and scattering characteristics of human benign prostatic hyperplasia tissue with Ti: sapphire laser irradiation in vitro. *Guang Pu Xue Yu Guang Pu Fen Xi* 2008;28(1):10–3.
- [23] Wei H-J, Xing D, Wu G-Y, Jin Y, Gu H-M. Optical properties of human normal small intestine tissue determined by Kubelka–Munk method in vitro. *World J Gastroenterol* 2003;9(9):2068–72.
- [24] Youn JI, Telenkov SA, Kim E, Bhavaraju NC, Wong BJ, Valvano JW, et al. Optical and thermal properties of nasal septal cartilage. *Lasers Surg Med* 2000;27(2):119–28.
- [25] Beek JF, Blokland P, Posthumus P, Aalders M, Pickering JW, Sterenborg HJ, et al. In vitro double-integrating-sphere optical properties of tissues between 630 and 1064 nm. *Phys Med Biol* 1997;42(11):2255–61.
- [26] Huang X, Jain PK, El-Sayed IH, El-Sayed MA. Gold nanoparticles: interesting optical properties and recent applications in cancer diagnostics and therapy. *Nanomedicine* 2007;2(5):681–93.
- [27] Rehman A, Firdous S, Nawaz M, Ahmad M. Optical parameters measurement for diagnostic and photodynamic therapy of human cervical adenocarcinoma (HeLa) cell line. *Laser Phys* 2011;22(1):322–6.
- [28] W. Poppendieck, Double integrating spheres: a method for assessment of optical properties of biological tissues, 2004.
- [29] Ritz JP, Roggan a, Germer CT, Isbert C, Müller G, Buhr HJ. Continuous changes in the optical properties of liver tissue during laser-induced interstitial thermotherapy. *Lasers Surg Med* 2001;28(4):307–12.
- [30] Skinner MG, Everts S, Reid AD, Vitkin IA, Lilge L, Sherar MD. Changes in optical properties of ex vivo rat prostate due to heating. *Phys Med Biol* 2000;1375(45):1375–86.
- [31] Alali S, Ahmad M, Kim A, Vurgun N, Wood MFG, Vitkin IA. Quantitative correlation between light depolarization and transport albedo of various porcine tissues. *J Biomed Opt* 2012;17(4):045004.
- [32] Yano T, Hatogai K, Morimoto H, Yoda Y, Kaneko K. Photodynamic therapy for esophageal cancer. *Ann Transl Med* 2014;2(3):29.
- [33] Racz E, Prens EP. Phototherapy and photochemotherapy for psoriasis. *Dermatol Clin* 2015;33(1):79–89.
- [34] Nau WH, Roselli RJ, Milam DF. Measurement of thermal effects on the optical properties of prostate tissue at wavelengths of 1064 and 633 nm. *Lasers Surg Med* 1999;24(1):38–47.
- [35] Agah R, Pearce JA, Welch AJ, Motamedi M. Rate process model for arterial tissue thermal damage: implications on vessel photocoagulation. *Lasers Surg Med* 1994;15(2):176–84.
- [36] Lewis RN, Mannock DA, McElhanev RN, Wong PT, Mantsch HH. Physical properties of glycosyldiacylglycerols: an infrared spectroscopic study of the gel-phase polymorphism of 1,2-di-O-acyl-3-O-(beta-D-glucopyranosyl)-sn-glycerols. *Biochemistry* 1990;29(38):8933–43.
- [37] Mannock DA, Collins MD, Kreichbaum M, Harper PE, Gruner SM, McElhanev RN. The thermotropic phase behaviour and phase structure of a homologous series of racemic beta-D-galactosyl dialkylglycerols studied by differential scanning calorimetry and X-ray diffraction. *Chem Phys Lipids* 2007;148(1):26–50.
- [38] Pressey JG, Pressey CS, Robinson G, Herring R, Wilson L, Kelly DR, et al. 2D-difference gel electrophoretic proteomic analysis of a cell culture model of alveolar rhabdomyosarcoma. *J Proteome Res* 2011;10(2):624–36.
- [39] De Pittà C, Tombolan L, Albiero G, Sartori F, Romualdi C, Jurman G, et al. Gene expression profiling identifies potential relevant genes in alveolar rhabdomyosarcoma pathogenesis and discriminates PAX3-FKHR positive and negative tumors. *Int J Cancer* 2006;118(11):2772–81.
- [40] Yang Z, MacQuarrie KL, Analau E, Tyler AE, Dilworth FJ, Cao Y, et al. MyoD and E-protein heterodimers switch rhabdomyosarcoma cells from an arrested myoblast phase to a differentiated state. *Genes Dev* 2009;23(6):694–707.
- [41] Beauvoit B, Evans SM, Jenkins TW, Miller EE, Chance B. Correlation between the light scattering and the mitochondrial content of normal tissues and transplantable rodent tumors. *Anal Biochem* 1995;226(1):167–74.